

## BER Performance of an Ultra-Wideband Impulse Radio Correlator Receiver

GIORGOS TATSIS, VASILIS CHRISTOFILAKIS, CONSTANTINOS VOTIS, PANOS  
KOSTARAKIS, LEONIDAS IVRISSIMTZIS, SPYRIDON K. CHRONOPOULOS

Physics Department  
University of Ioannina  
Panepistimioupolis, 45110  
GREECE  
gtatsis@grads.uoi.gr

*Abstract:* - This paper studies the characteristics of an Ultra-Wideband (UWB) communication system employing Impulse Radio techniques and, specifically, the effects of the matched filter of a correlator receiver in the performance of such a system. Such effects are evaluated in terms of the Bit Error Rate (BER) for a Binary Pulse Position Modulation (BPPM) scheme, in an indoor multipath propagation channel and in the presence of additive white Gaussian noise (AWGN). The case of imperfect channel estimation is taken into account, while comparisons with perfect channel estimation are performed. The dependence of BER on parameters such as the signal to noise ratio (SNR), the number of estimation pilot pulses and correlator taps, is finally derived. It is shown that there is an optimum number of correlator taps for best BER performance depending on the channel estimation procedure.

*Key-Words:* - Ultra-wideband, Impulse Radio, correlator, BER

### 1 Introduction

UWB communications have attracted considerable interest, targeting applications in high-speed data transfer wireless communication systems [1], [2]. A major benefit of such systems is the achievement of high data rates, with low power consumption and low system implementation cost. UWB systems are characterized as systems with spectral bandwidth greater than 500 MHz or with a fractional bandwidth greater than 20% [1]. One of the techniques employed in UWB communications is the Impulse Radio (IR), which uses trains of pulses of very short duration (of the order of a nanosecond). Due to the large bandwidth used, a special design in both transmitters and antennas is required [3], [4]. Various modulation schemes can thereafter be employed, including on-off keying (OOK), pulse amplitude modulation (PAM), pulse position modulation (PPM) and phase shift keying (PSK) [5], [6]. In this paper, for the purpose of the system performance characterization, BPPM is selected and equalization at the receiver is performed via the use of a filter matched to the waveform of pulses as they arrive at the receiver. BER calculation is carried out with the help of a simulation program, whereby the impact of propagation through the multipath channel is included, whilst imperfect channel estimation is

assumed. The article is organized as follows: Section 2 describes the signal model; in Section 3 we analyze theoretically the error probability; finally, in Section 4 numerical results are presented and discussed. The article is concluded in Section 5.

### 2 Signal Model Description

The transmitted pulses have the form of a Gauss monocycle, i.e. the first derivative of a standard Gauss pulse. Fig. 1 shows a schematic presentation of a BPPM modulated transmitted signal. The bit (frame) period corresponding to the period of data transfer is denoted by  $T_f$  and the time offset  $\Delta$  represents the modulation index.

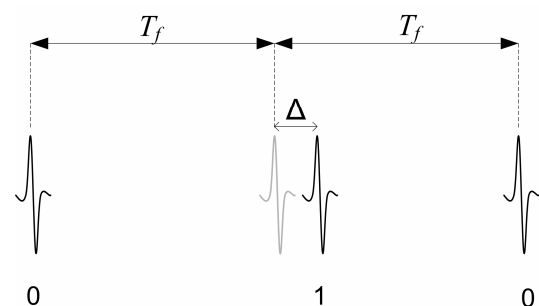


Fig.1 BPPM signaling

A logic “0” transmits a pulse at the nearest multiple of the period  $T_f$ , while sending a “1” is delayed in time by  $\Delta$  relative to the nearest multiple of  $T_f$ . Hence, the modulated pulses waveform  $s(t)$  can be expressed by

$$s(t) = \sum_{j=0}^{N-1} \sqrt{E_b} w(t - jT_f - b_j\Delta) \quad (1)$$

where  $w(t)$  is the pulse shape (first derivative of a Gaussian pulse) normalized to have unity total energy, i.e.  $\int_{-\infty}^{+\infty} |w(t)|^2 dt = 1$ ,  $E_b$  is the energy per bit,  $b_j$  is the  $j$ -th bit, and  $N$  is the total number of transmitted pulses. The form of the monocycle pulse is expressed by

$$w(t) = -At \exp\left(-\frac{t^2}{2\sigma_w^2}\right) \quad (2)$$

where  $A$  is the normalization factor and it can be found to equal to  $A = \sqrt{\frac{2}{\sigma_w^3 \sqrt{\pi}}}$ . On the other hand,  $\sigma_w$  is related to the pulse width via the relationship  $T_p = 2\pi\sigma_w$ , where  $T_p$  represents the width of the pulse, which encloses the 99.9% of the total pulse energy. The modulation index  $\Delta$  is chosen to satisfy the orthogonality property of the transmitted symbols, i.e.  $\int_{-\infty}^{+\infty} w(t)w(t-\Delta)dt = 0$ . We choose  $\Delta$  greater than the pulse duration, i.e.  $\Delta > T_p$ .

### 3 Theoretical Analysis

In order to evaluate the BER, we consider the transmission and reception system model shown in Fig. 2. The transmitted signal,  $s(t)$ , described above, propagates through a multipath channel with impulse response  $h(t)$ . Therefore, the signal at the receiver can be written as

$$r(t) = x(t) + n(t) = s(t) * h(t) + n(t) \quad (3)$$

where  $*$  denotes convolution and  $n(t)$  denotes AWGN. The noise has a mean value of zero and a double side power spectral density  $N_0/2$ , i.e.

$$n(t) \sim N(0, \sigma_n^2), \sigma_n^2 = \frac{N_0}{2}.$$

The channel impulse response is given by the IEEE 802.15.3a model [7], [8], and is expressed as follows:

$$h_i(t) = X_i \sum_l \sum_k \alpha_{k,l} \delta(t - T_l - \tau_{k,l}) \quad (4)$$

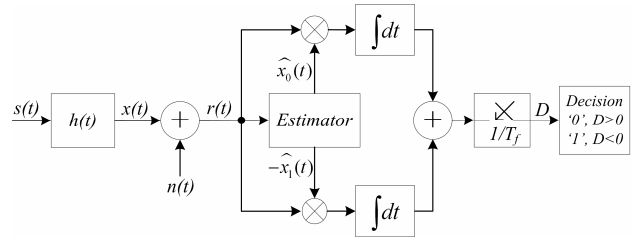


Fig.2 System transmission-reception model.

where  $k, l$  denotes the rays and clusters respectively,  $\alpha_{k,l}$  are the multipath gain coefficients,  $T_l$  is the delay of the  $l$ -th cluster,  $\tau_{k,l}$  is the delay of the  $k$ -th component relative to the  $l$ -th cluster,  $X_i$  represents the lognormal fading with  $i$  denoting the  $i$ -th channel realization. If we merge the delays of the paths we can describe the multipath channel more conveniently as

$$h(t) = \sum_{l=0}^{L-1} \alpha_l \delta(t - \tau_l) \quad (5)$$

where  $L$  is the number of resolvable paths,  $\alpha_l$  and  $\tau_l$  are the amplitude and delay of the  $l^{th}$  path, respectively, and  $\delta(t)$  is the Dirac delta function.

The matched filter in the receiver consists of a double correlator. The estimator of Fig. 2 presents the correlators with the template waveforms,  $\hat{x}_0(t)$  and  $\hat{x}_1(t)$ , which are the estimated received waveforms for transmitted bits “0” and bit “1”, respectively. The output of the correlators is sampled every  $T_f$  seconds and the decision metric ( $D$ ) defined by Eq. (11) below is compared with zero. We assume perfect time synchronization for reception and that there is no interference between sequential frames (IFI), thus the period  $T_f$  must be greater than the largest delay  $\tau_l$  of the channel. From this point on, and without loss of generality, we continue the process of reception of the first bit ( $0 < t < T_f$ ). The input signal in the matched filter is expressed as follows:

$$\begin{aligned} r(t) &= x(t) + n(t) = s(t) * h(t) + n(t) = \\ &= \sum_{l=0}^{L-1} \alpha_l s(t - \tau_l) + n(t) \end{aligned} \quad (6)$$

Prior to the correlation procedure, an estimation of the received waveform,  $x(t)$ , has to be performed. This is done by sending a number of pilot pulses carrying no information, e.g. only zeros.

In particular, if we transmit  $K$  pilot pulses, one every  $T_f$  seconds, then the estimated waveform is

obtained by averaging the received pulses. The template waveforms are respectively given by

$$\widehat{x}_0(t) = \frac{1}{K} \sum_{j=0}^{K-1} r_0^j(t) = \frac{1}{K} \sum_{j=0}^{K-1} (x_0^j(t) + n^j(t)) \quad (7)$$

and

$$\widehat{x}_1(t) = \widehat{x}_0(t - \Delta) \quad (8)$$

Assuming that the multipath channel is time-invariant during the estimation process and perfect synchronization, Eq. (7) becomes,

$$\widehat{x}_0(t) = x_0(t) + \frac{1}{K} \sum_{j=0}^{K-1} n^j(t) = x_0(t) + n_0(t) \quad (9)$$

The second term in the above equation  $n_0(t)$  is noise, normally distributed, with zero mean and variance  $\sigma_0^2 = \frac{1}{K^2} \sum_{j=0}^{K-1} \sigma_n^2 = \frac{\sigma_n^2}{K} = \frac{N_0}{2K}$ .

Similarly the estimated waveform for “1” is,

$$\widehat{x}_1(t) = x_0(t - \Delta) + n_0(t - \Delta) = x_1(t) + n_1(t) \quad (10)$$

The decision metric  $D$  in Fig. 2 can then be expressed as follows,

$$D = \int_0^{T_f} r(t) [\widehat{x}_0(t) - \widehat{x}_1(t)] dt = \int_0^{T_f} r(t) [x_0(t) - x_1(t) + n_x(t)] dt \quad (11)$$

where, the noise term  $n_x(t)$  is the total noise of the two correlators and has variance,

$$\sigma_x^2 = \sigma_0^2 + \sigma_1^2 = 2 \frac{N_0}{2K} = \frac{N_0}{K} \quad (12)$$

Hence, if a “0” is transmitted, the decision metric becomes

$$D = \int_0^{T_f} (x_0(t) + n(t))(x_0(t) - x_1(t) + n_x(t)) dt = M_0 + N_1 + N_2 + N_p \quad (13)$$

where,

$$M_0 = \int_0^{T_f} x_0(t)(x_0(t) - x_1(t)) dt$$

$$N_1 = \int_0^{T_f} (x_0(t) - x_1(t)) n(t) dt$$

$$N_2 = \int_0^{T_f} x_0(t) n_x(t) dt$$

$$N_p = \int_0^{T_f} n(t) n_x(t) dt$$

The terms  $N_1, N_2$  in Eq. (13) represent noise at the output of a linear filter and, hence, they are Gaussian r.v.’s defined as

$$N_1 \sim N(0, \sigma_{N_1}^2), \sigma_{N_1}^2 = \sigma_n^2 \int_{-\infty}^{+\infty} |x_0(t) - x_1(t)|^2 dt \quad (14)$$

$$N_2 \sim N(0, \sigma_{N_2}^2), \sigma_{N_2}^2 = \sigma_x^2 \int_{-\infty}^{+\infty} |x_0(t)|^2 dt \quad (15)$$

Since these two r.v.’s are independent and Gaussian distributed, their sum will also be a Gaussian r.v. with zero mean and variance equal to  $\sigma_{N_1}^2 + \sigma_{N_2}^2$ . In a vector representation, Eq. (13) can be written as

$$D = M_0 + N_g + N_p \quad (16)$$

where

$$M_0 = \mathbf{x}_0^T (\mathbf{x}_0 - \mathbf{x}_1)$$

$$N_g \sim N(0, \sigma_g^2),$$

$$\sigma_g^2 = \sigma_{N_1}^2 + \sigma_{N_2}^2 = \quad (17)$$

$$= \sigma_n^2 (\mathbf{x}_0 - \mathbf{x}_1)^T (\mathbf{x}_0 - \mathbf{x}_1) + \sigma_x^2 \mathbf{x}_0^T \mathbf{x}_0$$

$$N_p = \mathbf{n}^T \mathbf{n}_x = \sum_{i=1}^{L_x} n[i] n_x[i]$$

The discrete signals are considered to be the corresponding continuous-time waveforms sampled by an analog to digital converter. In our case no A/D errors are taken into account [9]., which is All vectors have length  $L_s$ , the number of channel paths with the strongest amplitude in the estimation process. In Eq. (17)  $(\cdot)^T$  denotes transpose. It should be pointed out that the random variable  $N_p$  is not Gaussian, but it represents a sum of products of independent Gaussian zero mean r.v.’s. Its probability density function (PDF) can be calculated numerically, [10], [11] and it is given by

$$p_e(x) = \frac{1}{\sigma_n \sigma_x (m-1)!} \times \exp\left(-\frac{|x|}{\sigma_n \sigma_x}\right) \sum_{i=0}^{m-1} \frac{(m+i-1)!}{2^{m+i} i! (m-i-1)!} \left(\frac{|x|}{\sigma_n \sigma_x}\right)^{m-1-i} \quad (18)$$

$$p_o(x) = \frac{\left(\frac{|x|}{2\sigma_n \sigma_x}\right)^m}{\sqrt{\pi} \Gamma(m + \frac{1}{2}) \sigma_n \sigma_x} K_m \left(\frac{|x|}{\sigma_n \sigma_x}\right)$$

where,  $\sigma_n = \sqrt{\frac{N_0}{2}}, \sigma_x = \sqrt{\frac{N_0}{K}}$  are the standard deviation of the random vectors  $\mathbf{n}$  and  $\mathbf{n}_x$ , respectively. The form of the PDF is different depending on  $L_s$  being even ( $p_e(x)$ ) or odd ( $p_o(x)$ ). In Eq. (18),  $\Gamma(\cdot)$  denotes the gamma

function and  $K_m(\cdot)$  is the modified Bessel function of the second kind of order  $m$ . Fig. 3. plots the PDF defined above for different values of  $L_s$ . For simplicity, we set  $\sigma_n = \sigma_x = 1$ . Note that when  $L_s$  is odd, the PDF is infinite for  $x=0$ . The mean value of  $N_p$  is clearly zero.

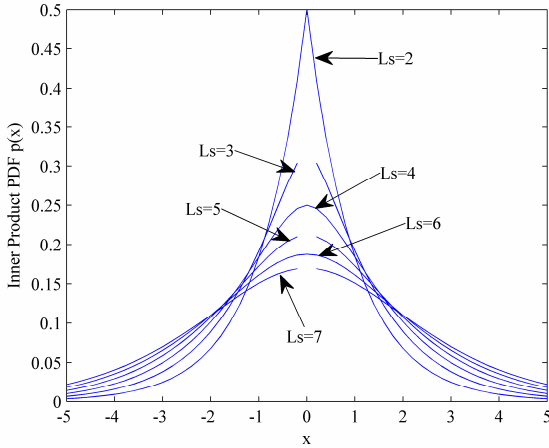


Fig.3 Probability Density Function for the sum of normal r.v.'s products  $p(x)$ , as defined in Eq. (18).

The decision metric is a r.v. with mean equal to  $M_0$ . The PDF of the total additive noise ( $N_g + N_p$ ), which determines the variance of the decision metric is the result of the convolution of the PDF of Eq. (18) and the Gaussian PDF,  $g(x)$ , namely

$$f(x) = g(x) * p(x) = \int_{-\infty}^{+\infty} g(x-z)p(z)dz \quad (19)$$

Then the probability of error when a “0” is transmitted is expressed as,

$$P_{e,0} = P(D < 0) = P(x < -M_0) = \int_{-\infty}^{-M_0} f(x)dx = \int_{M_0}^{+\infty} f(x)dx \quad (20)$$

where,  $M_0$  is defined by Eq. (17).

Similarly, the decision variable if “1” is transmitted can similarly be expressed as,

$$D = M_1 + N_g + N_p \quad (21)$$

where,

$$\begin{aligned} M_1 &= \mathbf{x}_1^T (\mathbf{x}_0 - \mathbf{x}_1) \\ N_g &\sim N(0, \sigma_g^2), \sigma_g^2 = \sigma_{N_1}^2 + \sigma_{N_2}^2 = \\ &= \sigma_n^2 (\mathbf{x}_0 - \mathbf{x}_1)^T (\mathbf{x}_0 - \mathbf{x}_1) + \sigma_x^2 \mathbf{x}_1^T \mathbf{x}_1 \\ N_p &= \mathbf{n}^T \mathbf{n}_x = \sum_{i=1}^{L_s} n[i]n_x[i] \end{aligned} \quad (22)$$

Evidently,  $M_1 = -M_0$  if we assume that the received symbol for “1” is not truncated at  $t = T_f$  which is the case if the frame period is sufficiently long, i.e.  $T_f > \max\{\tau_l\} + \Delta$ . Because of Eq. (8), we also have,  $\mathbf{x}_0^T \mathbf{x}_0 = \mathbf{x}_1^T \mathbf{x}_1$ , which means that the two symbols have the same energy and that the noise terms  $N_g$  in Eq. (16) and Eq. (21) have variance equal to  $\sigma_g$ . Similarly we can express the probability of error when an “1” is sent as follows,

$$P_{e,1} = P(D > 0) = P(x > |M_1|) = \int_{|M_1|}^{+\infty} f(x)dx = \int_{M_0}^{+\infty} f(x)dx \quad (23)$$

Hence, if ones and zeros are transmitted with equal probability and considering Eqs. (20) and (23), the BER is expressed as follows,

$$BER = \frac{1}{2} P_{e,0} + \frac{1}{2} P_{e,1} = \int_{M_0}^{+\infty} f(x)dx \quad (24)$$

Further, if we assume perfect channel estimation, the term  $n_x(t)$  in Eqs. (11) and (13) is zero. The total noise is, therefore, Gaussian with variance

$$\begin{aligned} \sigma_g^2 &= \sigma_n^2 \int_{-\infty}^{+\infty} |x_0(t) - x_1(t)|^2 dt = \\ &= \frac{N_0}{2} (\mathbf{x}_0 - \mathbf{x}_1)^T (\mathbf{x}_0 - \mathbf{x}_1) \end{aligned} \quad (25)$$

Thus, in case of perfect estimation, the BER is expressed as follows,

$$BER = Q\left(\frac{M_0}{\sigma_g}\right) \quad (26)$$

where,  $M_0$  is defined at Eq. (17).

## 4 Simulations and Numerical Results

The above analysis is carried out assuming constant, time-invariant channel parameters. The expressions (24) and (26) are, therefore, valid for a channel with constant associate parameters  $\alpha_{k,l}, \tau_{k,l}$  for the each path attenuation and delay. In order to obtain the error probability for time-varying, stochastic channel parameters, Eq. (4) is executed 1,000 times corresponding to different channel realizations, in order to obtain 1000 values of the BER. For each of the above runs we produce different random amplitudes and delays according to IEEE 802.15.3a model as defined in [5], [6]. The total BER, including small-scale fading, is thus obtained by averaging the 1000 different BERs with random channel parameters as described above.

For the simulations the channel model CM1 is selected. The pulse width is  $T_p = 300psec$  and the frame period  $T_f = 100nsec$ . The modulation index was set to  $\Delta = 1nsec$ . Fig. 4 shows the BER vs. the ratio  $E_b/N_0$  for various number of pilot pulses  $K$  in the case of imperfect channel estimation. In the same graph, the case of perfect estimation is shown for comparison. The number of correlator taps is  $L_s = 40$ . As we can see from Fig. 4, as the number of pilot pulses increase channel estimation becomes more precise and at large numbers, over 100, the estimation tends to be perfect. This is because the noise term in Eq. (13)  $n_x(t)$  has variance that is inversely proportional to  $K$  as defined by Eq. (12). The dependence of BER from  $K$  is shown in Fig. 5, for various values of  $E_b/N_0$  with  $L_s = 60$ . After a few tens (30-60) of pilot pulses, only a slight improvement in BER performance is achievable.

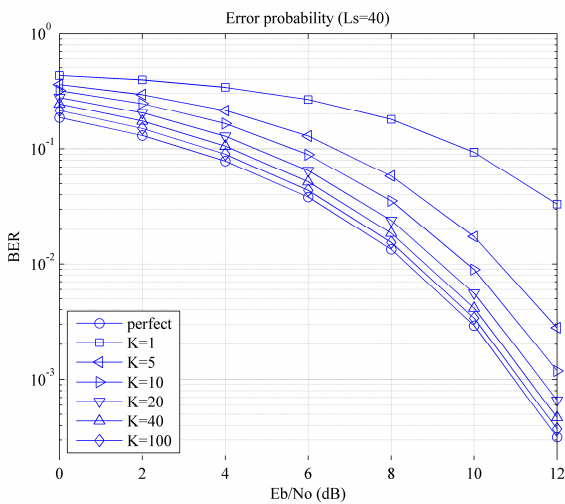


Fig.4 BER vs.  $E_b/N_0$  with different number of pilot pulses ( $K$ ) and in case of perfect channel estimation, with 40 correlation taps ( $L_s$ ).

Fig. 6 shows how the number of taps influences the BER, with several number of pilot pulses as a parameter. It is interesting to note that there is an optimum number of taps, for which BER is minimum, depending on the number of pilot pulses and this minimum value increases monotonically with  $K$ . This can be explained by examining Eq. (13). As the number of taps ( $L_s$ ) increases, the value of  $M_0$  also increases, resulting into a better SNR at the decision stage, if we consider only the noise term  $N_1$ . This is shown in the perfect estimation instance of Fig. 6. However, when the estimation is imperfect, the greater the number of taps the greater the variance of the noise terms

$N_2, N_p$ , which are strong enough to reduce the signal-to-noise ratio and result into a worse BER. However, this is the case when  $K$  is not significantly large.

Fig. 7 shows the BER as a function of the ratio  $E_b/N_0$  with  $L_s$  as parameter. At areas with low SNR (below 6dB), BER does not significantly improve by increasing the number of taps. In this case, we need as many pilot pulses ( $K$ ) as possible. In Fig. 7, 60 pulses were used. At a higher SNR, a greater number for taps may be required.

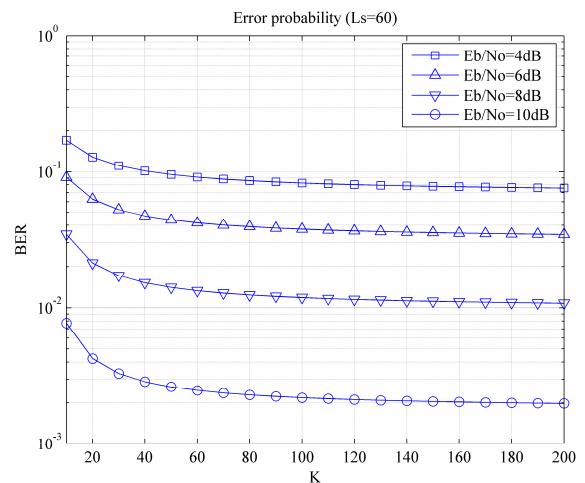


Fig.5 BER vs number of pilot pulses ( $K$ ) with 60 correlation taps ( $L_s$ ).

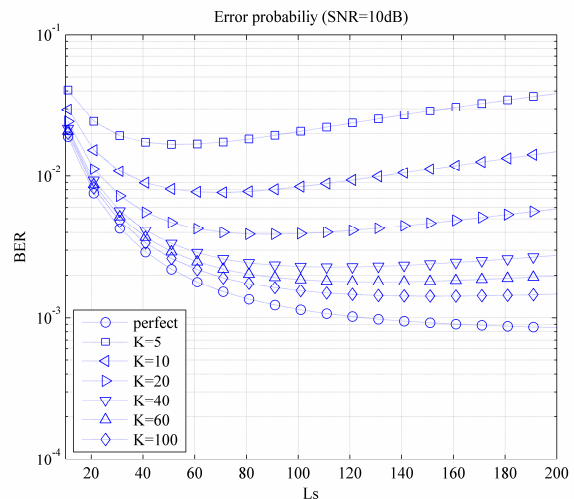


Fig.6 BER vs correlator taps ( $L_s$ ).  $E_b/N_0=10dB$ .

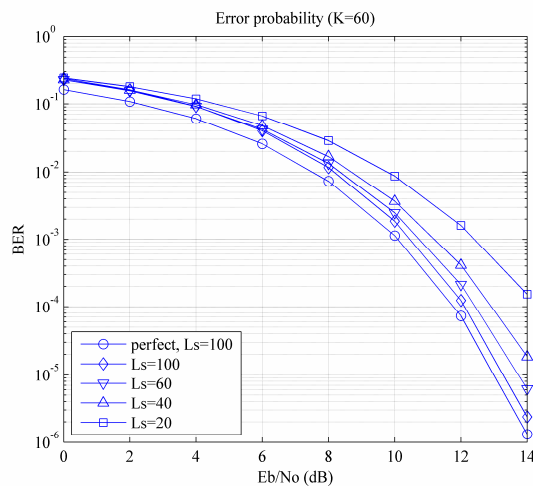


Fig.7 BER vs. Eb/No with different number of correlator taps in case of imperfect (K=60) and perfect estimation.

## 5 Conclusion

In this paper, the performance of a correlator receiver in UWB-IR systems was investigated. We evaluated the BER of such a system for the cases of perfect and imperfect channel estimation, focusing primarily into the second case. A simple channel estimation process has been described using a number of pilot pulses. Correlation is carried out using the strongest taps of the channel. We concluded that there is an optimum number of correlator taps that minimizes the BER of the system. Graphical representations of BER as a function of signal to noise ratio, correlator taps and pilot pulses for estimation were presented and discussed.

## 6 Acknowledgment

This research project (PENED) is co-financed by E.U.-European Social Fund (80%) and the Greek Ministry of Development-GSRT (20%).

### References:

[1] X. Shen, M. Guizani, R.C. Qiu, T. Le-Ngoc, "Ultra-wideband wireless communication and networks", Wiley 2006.  
 [2] Kazimierz Siwiak and Debra McKeown, "Ultra-Wideband Radio Technology", Wiley 2004.  
 [3] Giorgos Tatsis, Constantinos Votis, Vasilis Raptis, Vasilis Christofilakis, Spyridon K. Chronopoulos, Panos Kostarakis, "Design and Implementation of Ultra-Wideband Impulse Radio Transmitter", in Proceedings of 7th International Conference of Balkan Physical

Union (BPU), Alexandroupolis, Greece, September 9-13, 2009.

[4] Giorgos Tatsis, Vasilis Raptis, Panos Kostarakis, "Design and Measurements of Ultra-Wideband Antenna" International Journal of Communications, Network and System Sciences, Vol. 3, No. 2, Feb. 2010.  
 [5] Robert C. Qiu, Huaping Liu, Xuemin Shen, "Ultra-Wideband for Multiple Access Communications", IEEE, February 2005, pp 80-87.  
 [6] Ismail Güvenc, Hüseyin Arslan, "On the modulation options for UWB systems", IEEE 2003, pp. 892-897.  
 [7] Saleh and R. Valenzuela, "A Statistical Model for Indoor Multipath Propagation", IEEE JSAC, Vol SAC-5, No 2, Feb. 1987.  
 [8] Jeffrey R. Foerster, Marcus Pendergrass and Andreas F. Molisch, "A Channel Model for Ultrawideband Indoor Communication". Mitsubishi Electric Research Laboratory, Inc., TR-2003-73, November 2003.  
 [9] Giorgos Tatsis, Constantinos Votis, Vasilis Raptis, Vasilis Christofilakis, Panos Kostarakis, "A/D restrictions (errors) in Ultra-Wideband Impulse Radios", International Journal of Communications, Network and System Sciences, Vol. 3, No. 5, May 2010.  
 [10] Marvin K. Simon, "Probability Distributions Involving Gaussian Random Variables", Springer 2006, pp. 49-51.  
 [11] Andrew G. Glen, Lawrence M. Leemis, John H. Drew, "Computing the distribution of the product of two continuous random variables", Computational Statistics and Data Analysis 44 (3), pp. 451-464, 2004.